MORPHOLOGY AND FIELD RECOGNITION OF BAUXITE MINE FLOOR REGOLITH

Geoffrey A. Kew & Robert J. Gilkes

[1]School of Earth and Geographical Sciences, University of Western Australia,
35 Stirling Highway, Crawley, WA, 6009

INTRODUCTION

The recommended terminologies for deeply weathered profiles published by Anand & Paine (2002) do not adequately describe the various observed morphological properties of regolith materials remaining after mining of bauxitic laterite in the Darling Range of WA. The current terminology can not be used to identify relationships between physical properties and regolith material type. An improved classification of these materials is proposed that will aid in more effective rehabilitation of mine sites. This abstract discusses the morphology of regolith materials remaining after bauxite mining as described by scanning electron microscope and electron microprobe studies.

EXPERIMENTAL PROCEDURES

Trenches were excavated in mine floor materials after completion of bauxite mining at the Alcoa World Alumina Australia Huntly mine site. Intact clods were sampled and water retention and unconfined compression strength measurements determined (Kew & Gilkes 2005). Polished thin-sections of selected regolith materials were examined using a Nikon optical microscope under plane and cross-polarized light and the fabric components and their arrangements were documented. Backscattered electron imagesof polished sections were collected and electron microprobe and element maps were obtained using a Jeol 6400 scanning electron microscope.

RESULTS and DISCUSSION

Field-based morphological classification system

A field-based morphological classification system using hand texture, structure, colour and coarse fragment content was developed for regolith materials in the Darling Range, Western Australia (Table 1). The use of the term "zone" has been adopted to classify spatially complex assemblages of materials resulting from *in situ* isovolumetric weathering. Zones represent three dimensional bodies of material that differ in some respect from adjacent material. The definition of a zone relates to a part of the regolith having a distinct character, distinguishing it from adjacent parts of the regolith (Eggleton 2001).

Table 1: Regolith material classifcation system for Darling Range, Western Australia. Numbers 1, 2 and 3 indicate increasing clay content in Zm and Zp materials; increasing coarse fragment content in Zh materials; and both increasing clay content (first number) and coarse fragment content (second number) in Zg and Zd materials.

	Class	Subclass
Material appears loose or weakly structured		
Surface material	*A1*	
First overburden material	*A2*	
mixed topsoil and overburben material	*AZ*	
3D body of regolith material that remains after bauxite mining		
Mottled quartz rich material	*Zm*	Zm1 / Zm2 / Zm3
Pallid clay rich material	*Zp*	Zp1 / Zp2 / Zp3
Iron oxide cemented material	*Zh*	Zh1 / Zh2 / Zh3
Prior root channels	*Zr*	
Preserved granitic fabric material	*Zg*	Zg11 / Zg12 / Zg13 Zg21 / Zg22 / Zg23 Zg31 / Zg32 / Zg33
Preserved doleritic fabric material	*Zd*	Zd11 / Zd12 / Zd13 Zd21 / Zd22 / Zd23 Zd31 / Zd32 / Zd33 Zd31 / Zd32 / Zd33

Morphology

Electron microprobe analysis (EMPA) is presented in normalised ternary plots for % SiO_2, % Fe_2O_3 and % Al_2O_3 (Figure 2). Iron oxide cemented (Zh) materials (sample Zh3-Mu3-4) show distinct secondary mineral assemblages with characteristic “boxworks” of gibbsite present (spots 1 to 4) (% Al_2O_3 apex), goethite or

hematite (% Fe_2O_3 apex) and iron oxide cemented kaolin on the kaolin line (54% SiO_2 to Fe_2O_3 apex) (Figure 2). In contrast, EMPA of the matrix of quartz rich (Zm) material shows it to be composed of kaolin (spots 11-20) and small (< 10 μm) gibbsitic pseudomorph clasts after feldspar (spots 1-10) with no distinct groupings of minerals. The fractures within individual quartz grains are also composed of similar materials, but kaolin dominates when quartz fractures are approximately less than 30 μm. EMPA analysis of the matrix and kaolin booklets for clay rich (Zp) materials shows most points on or near the kaolin line. The quartz fracture fillings of clay rich (Zp) material are composed of kaolin in the form of small (< 30 μm) booklets.

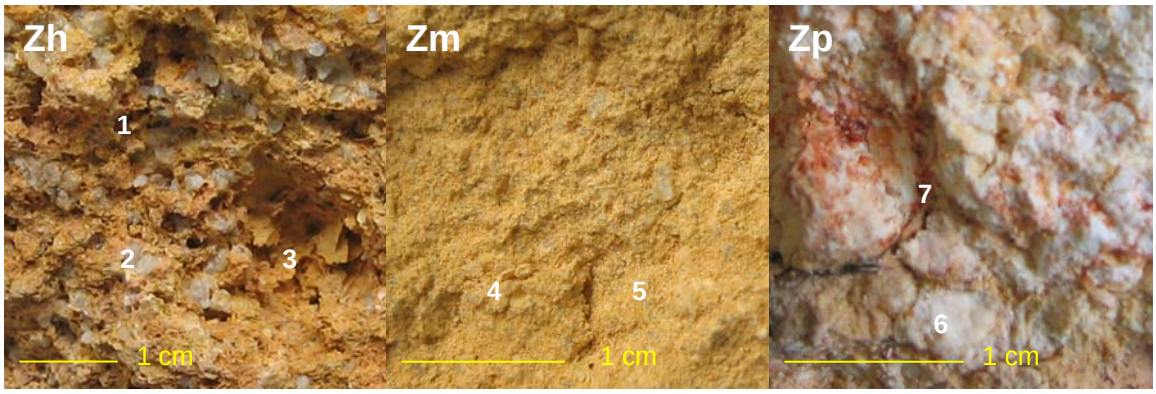

Figure 1: Dominant regolith material types derived from granitoid rock in the Darling Range, WA. Cemented red-brown iron oxide-rich material (Zh3), with voids (1), quartz (2) and septa (3) (bands of secondary minerals) formed along twinning planes or irregular cracks after weathering of primary minerals. Quartz rich (Zm3) material with low macroporosity (no cracks) and abundant quartz (4) in a ferruginous clay matrix (5). Clay rich material (Zp3) (mostly kaolinite and or halloysite) (6) with ped faces and cracks occupied by plant roots (7).

Elemental composition maps of Al and Si show the spatial distribution of these two elements within the matrix of quartz rich (Zm) and clay rich (Zp) materials. Subtraction of the Si map from the Al map (Al–Si) shows the distribution of gibbsite [$Al(OH)_3$] within the matrix (Figure 3). Silicon and Al are present in feldspar, biotite, chlorite, muscovite and kaolin or halloysite. Silicon is also present in kaolinite and quartz (SiO_2). Subtraction of the Si element map from the Al element map will leave Al)associated with these minerals as Si and Al occur in equal amounts in kaolinite. The bright areas remaining will be alumina rich and show the spatial distribution of gibbsite in the sample. The Al map for iron oxide cemented (Zh) materials is the same as that of the Al–Si map, indicating that gibbsite dominates in this material. The Al–Si map for quartz rich (Zm) materials gives scattered bright areas corresponding to a matrix composed of various mixtures of gibbsite and kaolin as shown by EMPA analysis. None or only minor bright areas are present in the Al–Si map for clay rich (Zp) materials indicating the matrix is composed predominately of kaolin.

Backscattered electron images at magnifications of 250 to 500 times, shows kaolin present adjacent to voids in quartz rich (Zm), clay rich (Zp) and preserved granitic fabric (Zg) materials, the latter being saprock. The origin of this kaolin has not been determined and may be the result of clay translocation or *in situ* weathering processes.

A sample of sandy clay loam quartz rich (Zm) material (sample Zm2-Mu3-8-2) showed distinct bands of Fe_2O_3 between kaolin, the tonal differences in the kaolin are associated with 10% or more Fe_2O_3 (from EMPA analysis after normalising for % Al_2O_3 + % SiO_2 + % Fe_2O_3 = 100%). The bright banding for Fe_2O_3 is associated with the porphyric fabric observed under the optical microscope (dark areas ppl) and also corresponds to the bright areas on the backscattered electron image. A silty clay loam clay rich (Zp) material (sample Zp2-Ch9-1) has kaolin deposited by water movement or formed from resilication of small (10 μm) clasts of gibbsite. The diameter of the void is in the mesopore range (30 μm or 0.3 mm) corresponding to a matric potential of 10 kPa (field capacity). This sample was collected from a depth of approximately 2 to 3m below the surface after mining and 7 to 8m prior to mining.

Water moves through this sized pore which is in the size range that is readily accessible to plant roots. The kaolin has also infilled mesopores (1 μm or 0.001 mm) between gibbsite clasts along the edge of the void up to a distance of approximately 20 μm. In this case, the process of kaolin formation or movement is associated with the void.

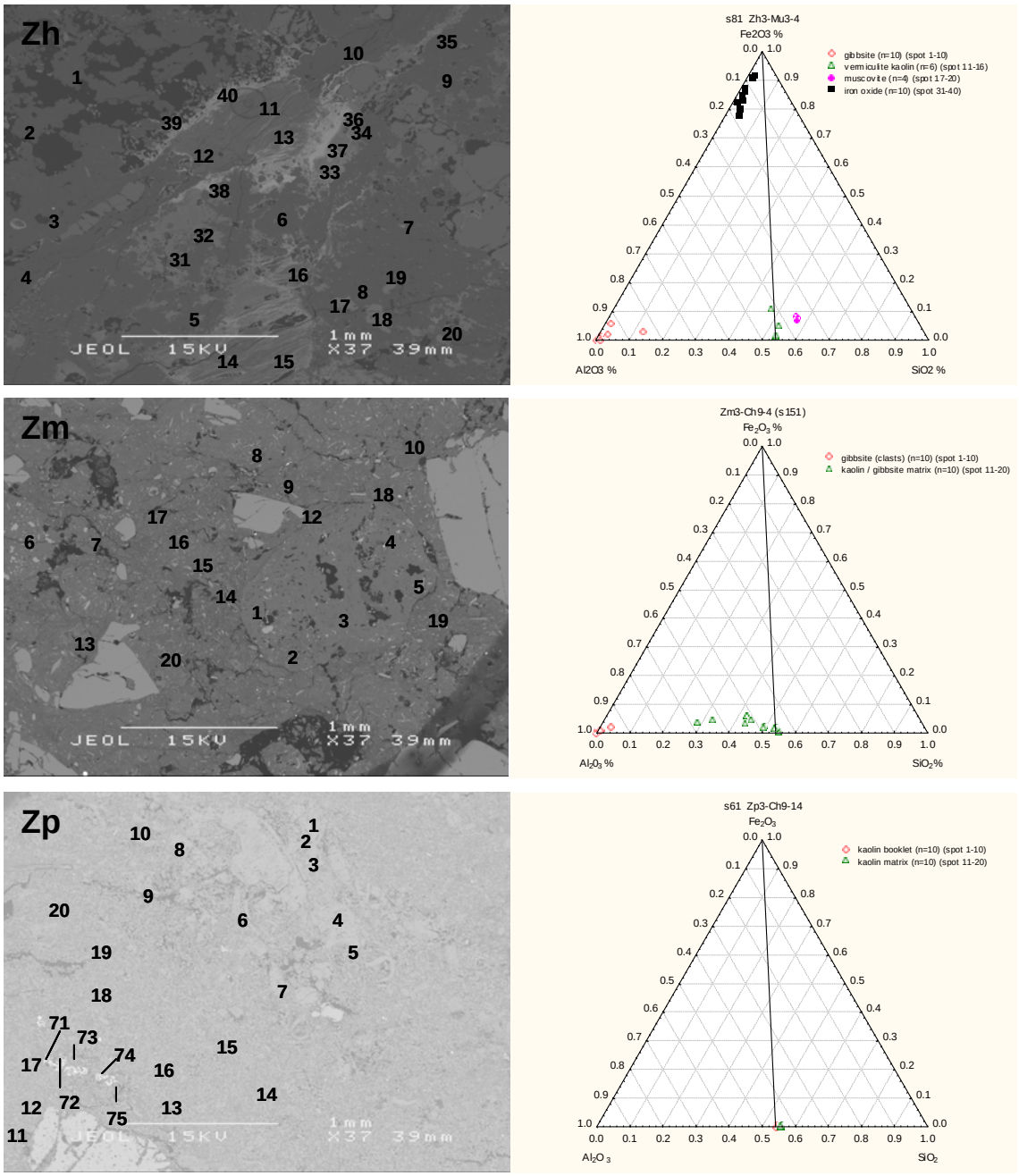

Figure 2: Backscattered electron images (BSE) and normalized ternary plots for cemented iron oxide (Zh), quartz rich (Zm) and clay rich (Zp) regolith materials. Numbers in BSE image correspond to spot analysis on ternary plots. Zh regolith shows distinct minerals with gibbsite, goethite or hematite and vermicular kaolin cemented by iron oxide. Quartz rich (Zm) material shows gibbsite clasts, with a matrix and quartz fractures composed of kaolin and gibbsite. Clay rich (Zp) material shows that matrix kaolin and kaolin booklets have the same chemical composition (sites 71 to 75 are anatase).

Kaolin associated with voids is also present in a preserved granitic fabric (Zg3) saprock sample (Zg3-Mu3-19). The kaolin is present within voids formed in feldspar grains, which also contain small (10 µm) clasts of gibbsite. The kaolin has a smooth surface indicative of flow, but has not infilled 1 µm mesopores as occurred in the clay rich (Zp) sample (Zp2-Ch9-1). An adjacent (within 2 mm) feldspar grain has altered to gibbsite along cleavage planes although the boundary of the mineral is still apparent. The origin and extent of kaolin movement needs further investigation including comparisons with thin sections of fresh rocks from the Darling Range.

Muscovite is more resistant to weathering than feldspar, biotite and chlorite in parent materials of bauxitic laterite in the Darling Range (Anand & Gilkes 1987). They found significant quantities of the muscovite in

adamellite which is a major granitic parent material at Huntly, Del Park and Jarrahdale mine sites and it has been retained in bauxite. Backscattered electron images of mine floor regolith of granitic origin from Huntly mine site show abundant muscovite. A sample of silty loam clay rich (Zp) material (Zp1-Ch9-8) from Chipala 9 mine site contained grains of muscovite showing iso-altermorph weathering (Delvigne 1998) to kaolin. Ternary plots of normalised percentages of K_2O, Al_2O_3 and SiO_2 show % K_2O for muscovite to be 6 to 8 % and for kaolin after muscovite 1 to 2 %. Muscovite fragments in regolith generally shows a two-fold larger size of longest axis in clay rich (Zp) material compared to quartz rich (Zm) materials which may have experienced greater pedoturbation. Muscovite in preserved granitic fabric materials is also twice as large as in clay rich (Zp) materials.

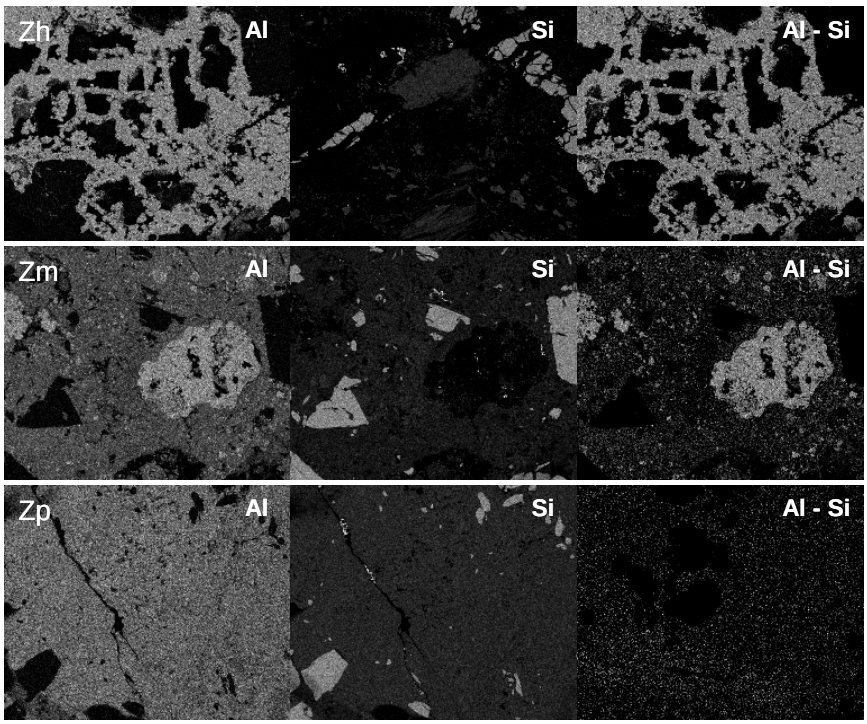

Figure 3: Aluminium (Al), silicon (Si) and Al minus Si (Al–Si) element maps for iron oxide cemented (Zh) material (sample Zh3-Mu3-2), sandy loam quartz rich (Zm) material (sample Zm3-Ch9-4) and silty clay loam clay rich (Zp) material (sample Zp2-Ch9-14, *maps are not available for sample Zp3-Ch9-14*). Bright areas on the Al–Si map indicate the spatial distribution of gibbsite. Zh materials are dominated by gibbsite, Zm materials have a matrix of both gibbsite and kaolin and Zp materials are dominated by kaolin.

Morphology and relationship to water retention, strength, ripping and root growth

The morphological classification system can be related to water retention and strength differences between regolith materials (Kew & Gilkes 2005). The total porosity of clay rich (Zp) materials was shown to be higher than for other materials. Dry and wet strength increases with clay content and the strength of grain supported fabrics (quartz rich Zm material) is more responsive to changes in water content than are matrix support fabrics (clay rich Zp material). The clay-water-clay bonding of the matrix is interrupted by the presence of quartz grains; Backscattered electron images and EMPA analysis show the presence of gibbsitic pseudomorph clasts after feldspar particularly in quartz rich (Zm) materials that are partly responsible for this interruption. This material should be targeted during rehabilitation ripping to encourage root growth.

REFERENCES

ANAND R.R. & GILKES R.J. 1987. Muscovite in Darling Range Bauxite Laterite. *Australian Journal Soil Research* **25**, 445-450.

ANAND R.R. & PAINE M. 2002. Regolith geology of the Yilgarn Craton, Western Australia: implications for exploration. *Australian Journal of Earth Sciences* **49**, 3-162.

DELVIGNE J.E. 1998. Atlas of micromorphology of mineral alteration and weathering. *The Canadian Mineralogist.* **Special publication 3.**

EGGLETON R.A. 2001. *The regolith glossary*. Cooperative Centre for Landscape Evolution and Mineral Exploration.

KEW G.A & GILKES R.J. in press. Strength and water retention characteristics of lateritic regolith. *Geoderma.*

Acknowledgements: We wish to acknowledge the assistance of Alcoa World Alumina Australia for access to the Huntly mine site, Dr C. Mathison from the School of Earth and Geographical Sciences, University of Western Australia for his assistance with thin section interpretation and the Centre for Microscopy and Microanalysis at UWA. We also wish to acknowledge funding from Alcoa World Alumina Australia and the Australian Research Council.